Alkanethiolate Self-Assembled Monolayers as Functional Spacers to Resist Protein Adsorption upon Au-Coated Nerve Microelectrode

Cheng-Hung Chang,[†] Jiunn-Der Liao,*[,‡] Jia-Jin Jason Chen,*[,†] Ming-Shaung Ju,[§] and Chou-Ching K. Lin[||]

Institute of Biomedical Engineering, Department of Materials Science and Engineering, Department of Mechanical Engineering, and Department of Neurology, National Cheng Kung University Hospital, National Cheng Kung University, No. 1, University Road, Tainan 70101, Taiwan

Received July 9, 2004

Alkanethiolate self-assembled monolayers (SAMs) of varied chain lengths were adsorbed upon Au-coated nerve microelectrodes and employed as protein-resistant spacers. The microelectrode spiraled as a cuff type can be used for restoring motor function via electrical stimulation on the peripheral nerve system; however, an increase of electrode impedance might occur during implantation. In this work, a thin-film SAMs treatment upon Au/polyimide (PI) surface of the microelectrode provided a hydrophobic characteristic, which retarded protein adsorption at the initial stage and subsequent pileup (or thickening) process. The protein-resistant effect exhibited comparable SAMs of different chain lengths adsorbed upon Au/PI surfaces. The increase of electrode impedance as a function of protein deposition time was mainly correlated with the addition of reactance that was associated with the pileup thickness of the deposited protein. Particularly, the SAMs-modified surface was capable to detach a significant portion of the accumulated protein from the protein-deposited SAMs/Au/PI, whereas the protein-deposited layers exhibited firm adhesion upon Au/PI surface. It is therefore very promising to apply thin-film SAMs adsorbed upon Au-coated surface for bioinvasive devices that have the need of functional electrical stimulations or sensing nerve signals during chronic implantation.

1. Introduction

Neural prostheses are devices that utilize electrical stimulation to activate the damaged or disabled nervous system for restoring motor and sensation functions. A fully implantable neural prosthesis usually consists of four components, namely, a functional microelectrode, stimulator/sensing amplifier, control system, and wireless telemetry module. By implanting such prostheses on the nerve trunk, biological signals can be acquired for sensory feedback[1,2] or the motor nerves[3,4] can be activated by electrical stimulation. Generally, the microelectrode acts as an insulating sleeve that can be placed around a length of nerve and utilized to sense the neural activities or to activate the damaged nervous system for function restoration.[5,6] Among various microelectrodes, nerve cuff microelectrodes have been applied in various neuroprosthetic applications, for example, the electrical stimulator for functioning the upper or lower extremity,[7,8] the diaphragm,[9] and the bladder[10] or for blocking the nerve transduction.[11,12]

The neuromuscular microelectrode can be sophisticatedly designed and fabricated using Micro-Electro-Mechanical System (MEMS) technique to measure neural activities.[13,14] It is a natural process that surface property of the implanted microelectrode is degraded as a function of time owing to the dynamic change of interfacial reactions.[15,16] For the nerve cuff-type microelectrode, there are two interfaces, namely, the interface between epineurium connected tissue and the inner surface of the cuff microelectrode and that between periprosthetic tissue and the outer part of the cuff microelectrode. It is desirable that the repairing periprosthetic tissue may glue on the outer surface of the cuff microelectrode to support the execution of nerve stimulation and proximal muscle movement. Unlike the contact with central nervous system, the surface of inner cuff microelectrode is preferably nonadhered to protein and cells of the peripheral

* Corresponding authors. J.-D. Liao: e-mail: jdliao@mail.ncku.edu.tw; tel: 886 6 2757575 ext. 62971; fax: 886 6 2346290. J.-J. J. Chen: e-mail: jason@jason.bme.ncku.edu.tw.

[†] Institute of Biomedical Engineering.

[‡] Department of Materials Science and Engineering.

[§] Department of Mechanical Engineering.

[||] Department of Neurology.

(1) Haugland, M. K.; Lickel, A.; Haase, J.; Sinkjaer, T. *IEEE Trans. Rehabil. Eng.* **1999**, *7*, 215.

(2) Haugland, M. K.; Hoffer, J. A. *IEEE Trans. Rehabil. Eng.* **1994**, *2*, 29.

(3) Aoyagi, Y.; Mushahwar, V. K.; Stein, R. B.; Prochazka, A. *IEEE Trans. Rehabil. Eng.* **2004**, *12*, 1.

(4) Stieglitz, T.; Schuettler, M.; Schneider, A.; Valderrama, E.; Navarro, X. *IEEE Trans. Rehabil. Eng.* **2003**, *11*, 427.

(5) Rutten, W. L. C.; Smit, J. P. A.; Frieswijk, T. A.; Bielen, J. A.; Brouwer, A. L. H.; Buitenweg, J. R.; Heida, C. *IEEE Eng. Med. Biol.* **1999**, *18*, 47.

(6) Wise, K. D.; Anderson, D. J.; Hetke, J. F.; Kipke, D. R.; Najafi, K. *IEEE Proc.* **2004**, *92*, 76.

(7) Smith, B. T.; Mulcahey, M. J.; Betz, R. R. *IEEE Trans. Rehabil. Eng.* **1996**, *4*, 264.

(8) Fujita, K.; Handa, Y.; Hoshimiya, N.; Ichie, M. *IEEE Trans. Rehabil. Eng.* **1995**, *3*, 360.

(9) Schmit, B. D.; Mortimer, J. T. *IEEE Trans. Rehabil. Eng.* **1999**, *7*, 150.

(10) Boyer, S.; Sawan, M.; Abdel-Gawad, M.; Robin, S.; Elhilali, M. M. *IEEE Trans. Rehabil. Eng.* **2000**, *8*, 464.

(11) Tai, C.; Jiang D. *IEEE Trans. Biomed. Eng.* **1994**, *41*, 286.

(12) Van Den Honert, C.; Mortimer, J. T. *IEEE Trans. Biomed. Eng.* **1981**, *28*, 373.

(13) Najafi, K. *MHS'95. Proc.* **1995**, *4*, 11.

(14) Cheung, K. C.; Djupsund, K.; Dan, Y.; Lee, L. P. *J. Microelectromech. Syst.* **2003**, *12*, 179.

(15) Rosengren, A.; Wallman, L.; Danielsen, N.; Laurell, T.; Bjursten, L. M. *IEEE Trans. Biomed. Eng.* **2002**, *49*, 392.

(16) Peterson, D. K.; Nochomovitz, M. L.; Stellato, T.A.; Mortimer, J. T. *IEEE Trans. Biomed. Eng.* **1994**, *41*, 1115.

10.1021/la040097t CCC: $27.50
Published on Web 11/24/2004

nerve to deliver the stimulation current to the nerve axons or to receive the action potential signal from axons.[17]

The performance of electrical stimulation using the functional microelectrode is influenced by many factors. Among them, the loss of electrical power owing to the increase of electrode impedance is the most relevant. The power loss factor should be as low as possible and also stable when the microelectrode wraps around the nerve trunk or adheres to the peripheral tissue. The most influential factor may come from the increase of electrode impedance at the interface between the nearby epineurial connective tissue and the inner surface of the cuff microelectrode. As the nerve microelectrode becomes sheathed, its electrode impedance increases, which may result in a deficiency in nerve stimulation or signal recording.[18] The microelectrode combined with other components as an invasive device should follow the criterion for implantable materials, which are not physically or chemically harmful to the peripheral nerves during long-term implantation.[19] The excessive scar tissues or adsorbed protein are unavoidably formed on the surfaces of the cuff-type microelectrode and naturally increased as a function of implantation time. Therefore, means to slow the increased rate of electrode impedance is a vital task to extend the lifetime of the functional microelectrode. The kinetics of interfacial reactions between the surface of the microelectrode and the epineurium is therefore decisive in assessing the characteristic of functional cuff microelectrode, as well as the neural prosthesis.

Surface modification on the functional microelectrode is a well-recognized tool to promote its performance of electrical measurements. Recent biomimetic design using long chains of extracellular matrix protein as bioactive molecules aims to promote cell adhesion or induce cell proliferation.[20] This type of modification considerably improves the fixation of an implanted microelectrode. For isolating purpose on the inner surface of microelectrode, a tightly adhered layer to the metallic substrate might have the following requirements: without voids at the interface, insulating coating with considerable uniformity in thickness over all the metallic substrate, and thermal and biological stability when functioning.

There are various chemical species utilized for surface modification of implantable devices. For example, the synthesized poly(ethylene glycol) (PEG) was introduced on the iridium-made pacemaker electrodes,[21] and a tailored modification using alkanethiolate self-assembled monolayers (SAMs) on Au-coated surface was achieved.[22,23] Both treatments provide a hydrophobic surface capable to prevent the exposed surface of the microelectrode from protein adsorption or cell adhesion and therefore to lessen the increase of electrode impedance.[20] The former method has been described as the "steric mechanics" in a physiological fluid environment, while the grafted PEG acts as a "brush" to remove protein or cells from the surface.[24] The physiological environment in contact with nerve tissue exhibits relatively dehydrated, therefore a thin-film surface with lasting hydrophobic and nonadhering properties should be appropriate as an exterior of the bioinvasive device for stimulating the peripheral nerve and sensing the nerve signals. The latter treatment method using $-CH_3$ as the tail group leads to close-packed arrays of amphipilic molecules, which are chemically adsorbed upon Au-coated surface. Considering the practical aspect, of the thin-film SAMs, that the headgroup of an adsorbate covalently bonds to a solid substrate (e.g., S−Au) while the chainlike molecular tail of $-CH_3$ sticks out from the substrate provides a means to tailor the surface as a hydrophobic or nonadhesive property.[25,26] It is therefore very convenient to introduce such alkanethiolate structure as tail group on SAMs[24−26] and to investigate the interactions between biological objects and SAMs with the tail group.

The MEMS-fabricated microelectrodes have become the main stream for the implantable microelectronic device.[27] Usually, the implanted microelectrode functions normally within a few weeks; thereafter, the exposed surfaces of the microelectrode to the periprosthetic tissue are coated with scar tissues during semiacute or chronic implantation. In this study, the alkanethiolate SAMs adsorbed upon Au-coated microelectrode surface are expected to play one part to stimulate the peripheral nerve and the other part to distinguish the neural signal from the feedback signals. This work aims to reduce protein adsorption and cells adhesion on the SAMs-modified surface of the novel multipolar spiral cuff microelectrode. A means likely to extend the lifetime of the functional microelectrode is also proposed.

2. Materials and Methods

2.1. Fabrication of Multipolar Spiral Cuff Microelectrode. The multipolar nerve microelectrodes were manufactured in a clean room on 4-in. silicon wafer using MEMS technique,[28] developed at the Southern Taiwan MEMS Center, National Cheng Kung University. Figure 1a demonstrates the structure of multimicroelectrodes, which consisted of 12 nerve contact electrodes and binding pads (Figure 1b). Each thin-film unit containing nine multipolar microelectrodes shown in Figure 2a could be cut from the wafer. The thin-film multipolar microelectrode was linked to a connector and an external monitoring device, and thereafter the microelectrode was spiraled as a cuff type (Figure 2b) for further in vitro study.

2.2. Surface Modification of Au Substrate. There were two kinds of Au-coated substrates. One was prepared by electron beam evaporation of ≈200 nm of Au on Ti-primed (≈20 nm) polished single-crystal Si(100) wafers (Silicon Sense). The resulting metal films are polycrystalline, with a grain size of 20∼50 nm as observed by atomic force microscopy (AFM). The grains predominantly exhibit an (111) orientation, which is also corroborated by the observation of the corresponding forward-scattering maxima in the angular distributions of the Au 4f photoelectrons[29] and by the characteristic binding energy (BE) shift of the Au 4f surface core level.[30] The other was a Au film prepared by electron beam evaporation on the biocompatible polyimide (PI) substrate for the multipolar spiral cuff microelectrode.

(17) Grill, W. M.; Mortimer, J. T. *J. Biomed. Mater. Res.* **2000**, *50*, 215.
(18) Branner, A.; Stein, R. B.; Fernandez, E.; Aoyagi, Y.; Normann, R. A. *IEEE Trans. Biomed. Eng.* **2004**, *51*, 146.
(19) Rousche, P. J.; Pellinen, D. S.; Pivin, D. P.; Williams, J. C.; Vetter, R. J. *IEEE Trans. Biomed. Eng.* **2001**, *48*, 361.
(20) Mrksich, M.; Whitesides, G. M. *Annu. Rev. Biophys. Biomol. Struct.* **1996**, *25*, 55.
(21) Stelzle, M.; Wagner, R.; Jagermann, W. *IEEE Proc. EMBS'96* **1996**, *1*, 114.
(22) Himmel, H. J.; Weiss, K.; Jaeger, B.; Dannenberger, O.; Grunze, M.; Woell, C. *Langmuir* **1997**, *13*, 4943.
(23) Jung, C.; Dannenberger, O.; Buck, M.; Grunze, M. *Langmuir* **1998**, *14*, 1103.
(24) Gupta, A. K.; Wells, S. *IEEE Trans. NanoBioscience* **2004**, *3*, 66.
(25) Dubois, L. H.; Nuzzo, R. G. *Annu. Rev. Phys. Chem.* **1992**, *43*, 437.
(26) Whitessides, G. M.; Gorman, C. B. *Handbook of Surface Imaging and Visualization: Self-Assembled Monolayers: Models for Organic Surface Chemistry*; CRC Press: Boca Raton, FL, 1995; pp 713−732.
(27) Grayson, A. C. R.; Shawgo, R. S.; Johnson, A. M.; Flynn, N. T.; Yawen L. I.; Cima, M. J.; Langer, R. *IEEE Proc.* **2004**, *92*, 6.
(28) Ju, M.-S.; Chien, H.-C.; Chen, G.-S.; Lin, C.-C. K.; Chang, C.-H.; Chang, C.-W. *Chinese J. Med., Biol. Eng.* **2002**, *22*, 33.
(29) Nam, Y.; Chang, J.-C.; Wheeler, B. C.; Brewer, G. J. *IEEE Trans. Biomed. Eng.* **2004**, *51*, 158.
(30) Kohn, F. Diploma Thesis, Universität Heidelberg, Heidelberg, Germany, 1998.

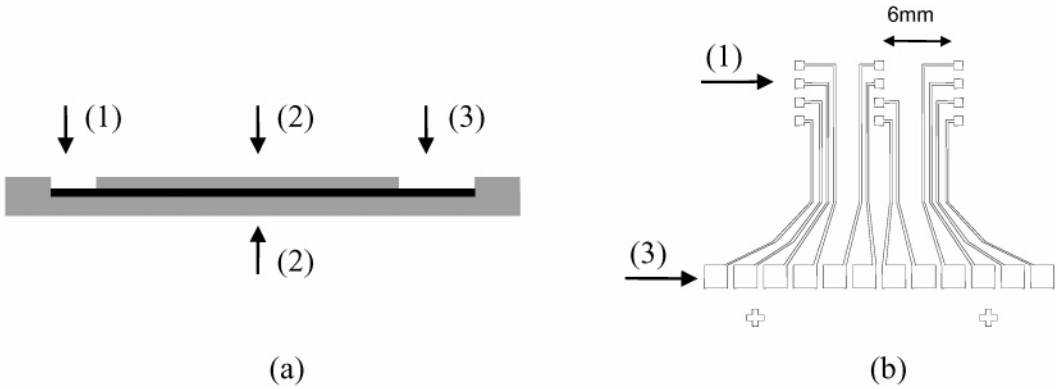

Figure 1. (a) The microelectrodes were composed of Au-coated layout sandwiched in a flexible PI-insulated substrate that the photosensitive PI film of 15-μm thickness was utilized as the substrate for the deposition of Au layer (2500 Å prepared by electron beam evaporation) and subsequent spin-coated PI film of 10-μm thickness as an insulator upon the microelectrode surface. (b) An enlarged, single multi-microelectrode consisted of 12 nerve contact electrodes (800 μm × 800 μm). The measuring distance between nerve contact electrodes was 6 mm.

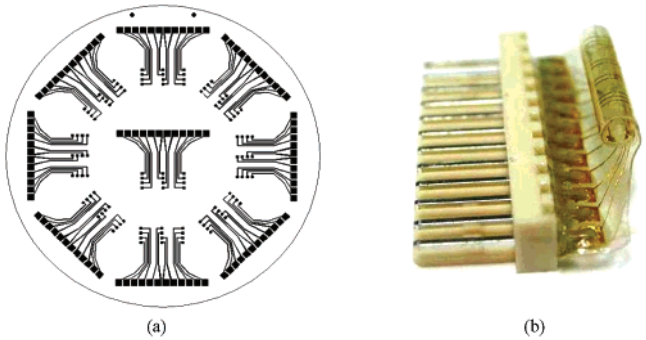

Figure 2. The multipolar nerve microelectrodes were manufactured in a clean room on 4-in. silicon wafer using MEMS technique. (a) The finished microelectrode contained nine multipolar microelectrodes and then (b) linked to a connector and an external monitoring device.

The SAMs of different alkyl chain lengths (Fluka Chemicals) were utilized. The 1-dodecanethiol ($C_{12}H_{26}S$, DDT), 1-hexadecanethiol ($C_{16}H_{34}S$, HDT), and 1-octadecanethiol ($C_{18}H_{38}S$, ODT) with sulfur anchor group were chemisorbed upon Au/Ti/Si as well as Au/PI (before spiraled as a cuff-type microelectrode) surfaces in an ethanolic 1 mM solution in a desiccator for 24 h. After the immersion, the microelectrodes were carefully rinsed and cleaned with ethanol and blown with pure dry argon. The PI surface was O_2 plasma-treated for ≈20 s before Au deposition for a firm adhesion upon PI surface, which significantly avoided the Au/PI boundary from peeling during SAMs treatment.

2.3. Sample Characterization by Contact Angle Measurement. Water contact angles were measured immediately after preparing the SAMs-modified samples. The measurements were performed under argon atmosphere at 22 ± 1 °C. The sessile drop method was used and a JVC-TK1200 microscope with processing software took the droplet image. For each sample, 10 measurements with a standard deviation below 1° were carried out and an average value was calculated.

2.4. Chemistry of the Modified Surface. Using synchrotron-based high-resolution X-ray photoelectron spectroscopy (HRXPS), the chemical structures of Au/Ti/Si and Au/PI samples with different SAMs treatments were characterized. Measurements were carried out at the U5 undulatory beam line of the National Synchrotron Radiation Research Center in Hsinchu, Taiwan. The time for the acquisition of the entire set of the HRXPS spectra for an individual sample was selected as a compromise between the spectra quality and a damage induced by X-rays.[30] The spectra were fitted using Voigt peak profiles and a Shirley background. Detail of the equipment and the processing parameters can be found elsewhere.[31−34]

2.5. Protein Adsorption along Time and Protein Detachment Test. Blood plasma was obtained from 2∼3 kg male New Zealand white rabbits by centrifuging at 160 g for 10 min and diluting to 1:3 with saline solution (i.e., 0.9% NaCl in D. I. water, pH value ≈7.0). The diluted blood plasma was heated to 37 °C and incubated with Au/PI or SAMs/Au/PI film of the cuff microelectrode at 100% humidity. At the end of the incubation period, samples were taken out, shortly washed with D. I. water, and dried overnight in a desiccator. The scanning probe microscope (NT-MTD SPM, Russia) was applied to examine the topographic images of protein-adsorbed layers. The silicon tip in contact mode was used, while the scan area was set to 20 μm by 20 μm for all samples.

For protein detachment test, the 14-day protein-deposited samples were slightly rinsed using deionized water and dried in a desiccator. Subsequently, a stereomicroscope (Nikon SMZ-2T) was employed to estimate the fractional coverage of residual protein upon the tested surface, which indicated its affinity to the primarily deposited protein.

2.6. Measurement of AC Impedance for the Cuff Microelectrode. The in vitro assessments of the multi-microelectrodes were performed by measuring the AC impedance of Au/PI or SAMs/Au/PI in contact with saline solution containing diluted blood plasma at room temperature. Total impedance, resistance, and reactance of the multipolar microelectrode were measured by an LCR analyzer (Agilent 4294A precision LCR analyzer); the testing frequencies were in the range of 40 Hz∼15 kHz with a total 200 points of each scan. The testing signal amplitude was 5 mV rms (AC). Data analyses were processed using MATLAB V6.5 software offline. Practical guidelines from Agilent were referenced to select a circuit mode suitable for electrode impedance measurement.

3. Results and Discussion

3.1. Pristine SAMs/Au Surfaces. The C 1s, S 2p, N 1s, and O 1s HRXPS spectra of DDT/Au/Ti/Si, HDT/Au/Ti/Si, ODT/Au/Ti/Si, and ODT/Au/PI surfaces are presented in Figure 3. For the SAMs/Au/Ti/Si surfaces, their C 1s spectra exhibited a single emission peak at a BE of 284.8 eV with an fwhms of ≈0.9 eV in good agreement with Heister el al.[35] No traces of oxygen or nitrogen were found. For the analogous surfaces, the S 2p spectrum exhibited a single S 2p doublet with a BE of ≈162.0 eV for the S $2p_{3/2}$ component. This doublet is commonly related to the thiolate species bonded to Au surface.[31,36] No traces of other sulfur-derived species such as atomically adsorbed

(31) Heister, K.; Zharnikov, M.; Grunze, M.; Johansson, L. S. O. *J. Phys. Chem. B* **2001**, *105*, 4058.

(32) Liao, J.-D.; Wang, M.-C.; Weng, C.-C.; Klauser, R.; Frey, S.; Zharnikov, M.; Grunze, M. *J. Phys. Chem. B* **2002**, *106*, 77.

(33) Wang, M.-C.; Liao, J.-D.; Weng, C.-C.; Klauser, R.; Frey, S.; Zharnikov, M.; Grunze, M. *J. Phys. Chem. B* **2002**, *106*, 6220.

(34) Wang, M.-C.; Liao, J.-D.; Weng, C.-C.; Klauser, R.; Shaporenko, A.; Grunze, M.; Zharnikov, M. *Langmuir* **2003**, *19*, 9774.

(35) Heister, K.; Zharnikov, M.; Grunze, M.; Johannson, L. S. O.; Ulman, A. *Langmuir* **2001**, *17*, 8.

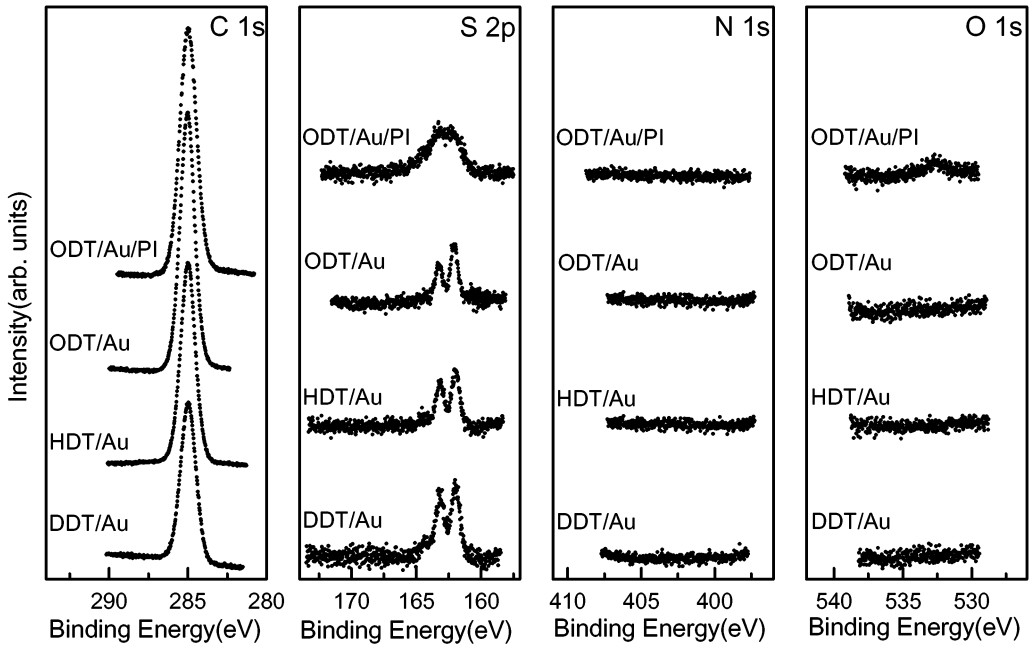

Figure 3. C 1s, S 2p, N 1s, and O 1s HRXPS spectra of different surfaces: DDT/Au/Ti/Si, HDT/Au/Ti/Si, ODT/Au/Ti/Si, and ODT/Au/PI (from bottom to top).

sulfur[37,38] or irradiation-induced dialkylsulfide species[31] were found. In ODT/Au/PI, a worse surface quality resulted from Au deposition upon PI, rather than a well-ordered metal substrate. Thereafter, the ODT molecules were adsorbed upon such Au/PI surface, from which an inferior S 2p and O 1s spectra were obtained. Analogous spectra were found on the DDT/Au/PI and HDT/Au/PI surfaces (not shown). Overall, the SAMs/Au/PI surfaces contained a small portion of debonded S−Au (BE ≈ 163.2 eV) that might slightly alter the characteristics of the thin-film SAMs.

Water contact angles of the pristine Au, DDT/Au, HDT/Au, and ODT/Au on Ti/Si surfaces were around 58°, 96°, 104°, and 107°, respectively.[34] The increase of contact angle was roughly expected for the variation of chain lengths and the hydrophobic CH_3 surface, namely, the tail group of the alkanethiolate SAMs. For the SAMs/Au/PI surfaces, their contact angles were insignificantly changed.

In our previous studies,[32,33] the structure and spacing of the aliphatic monomolecular film on Au(111) surface were calculated as a c(4 × 2)rect modulated ($\sqrt{3} \times \sqrt{3}$)R30° lattice with a spacing of ≈5 Å between the alkanethiolate adsorbates. Within these 2D lattices, the tilt angle of the alkanethiolates was ≈30° on Au(111) surface with approximately the same bulk density for the alkanethiolate SAMs/Au. On the basis of this estimation, the SAMs film thickness was calculated to be around 15.0 Å, 19.4 Å, and 21.6 Å for DDT, HDT, and ODT, respectively. Assume that the spacing and bulk density for analogous headgroup (Au−S) were comparable for the SAMs/Au/PI surfaces; the major difference among such SAMs structures was therefore correlated with their alkyl chain lengths.

3.2. Measurement of AC Impednce for the Cuff Microelectrode. Figure 4 exhibited the impedance measurement on the Au/PI or SAMs/Au/PI surface of the microelectrode. According to the Agilent guidelines and our experimental measurement, the parallel circuit mode illustrated in Figure 4a was selected for the cuff-type microelectrode when immersed into saline solution containing diluted blood plasma. For the parallel circuit mode, the capacitance is expected to be small regardless of any electrical double layer model used to interpret the results. Small capacitance yields large reactance (Ci), which implies that the effect of the parallel resistance (Ri) has relatively more significance than that of series resistance (Rs). In the experiment, the total impedances for Au/PI samples without or with SAMs treatment versus testing days were measured at 1 kHz and are shown in Figure 4b. Their respective resistance and reactance were decomposed and are presented in Figure 4c and 4d. Compared with the selected parallel circuit mode, the resistance of saline solution containing diluted blood plasma was of insignificance, whereas the measurement of total impedance corresponded well with that of reactance.

The measured frequency of 1 kHz was placed within the so-called "suitable" frequencies in the range of 0.5∼1.5 kHz (i.e., the frequencies in the * region shown in Figure 5), which received their total impedances above ≈10 KΩ. In Figure 4b, the total impedances as measured were also higher than ≈10 KΩ; the value is a rule of thumb for selecting the parallel circuit mode. The selection of "suitable" frequencies was chiefly based upon (1) the signals spectrum of nerve being recorded in the range of 0.5∼3.0 kHz, (2) the stimulation of the peripheral nerve being applied in the range of 10 Hz∼2.0 kHz, and (3) the sensitivity of electrode impedance measurement, that is, the difference of impedance between SAMs/Au/PI and Au/PI samples.

From the relations of the respective impedances as a function of testing days for different microelectrode surfaces, presented in Figure 4b−d, their increasing tendency was roughly comparable. The increase of electrode impedance was mainly correlated with the addition of reactance, whereas the resistance was insignificantly changed. It implied that the cause of increasing impedance on the microelectrode surface particularly resulted from

(36) Heister, K.; Rong, H.; Buck, M.; Zharnikov, M.; Grunze, M.; Johansson, L. S. O. *J. Phys. Chem. B* **2001**, *105*, 6888.

(37) Himmelhaus, M.; Gauss, I.; Buck, M.; Eisert, F.; Wöll, C.; Grunze, M. *J. Electron Spectrosc.* **1998**, *92*, 139.

(38) Hutt, D. A.; Leggett, G. J. *J. Phys. Chem. B* **1996**, *100*, 6657.

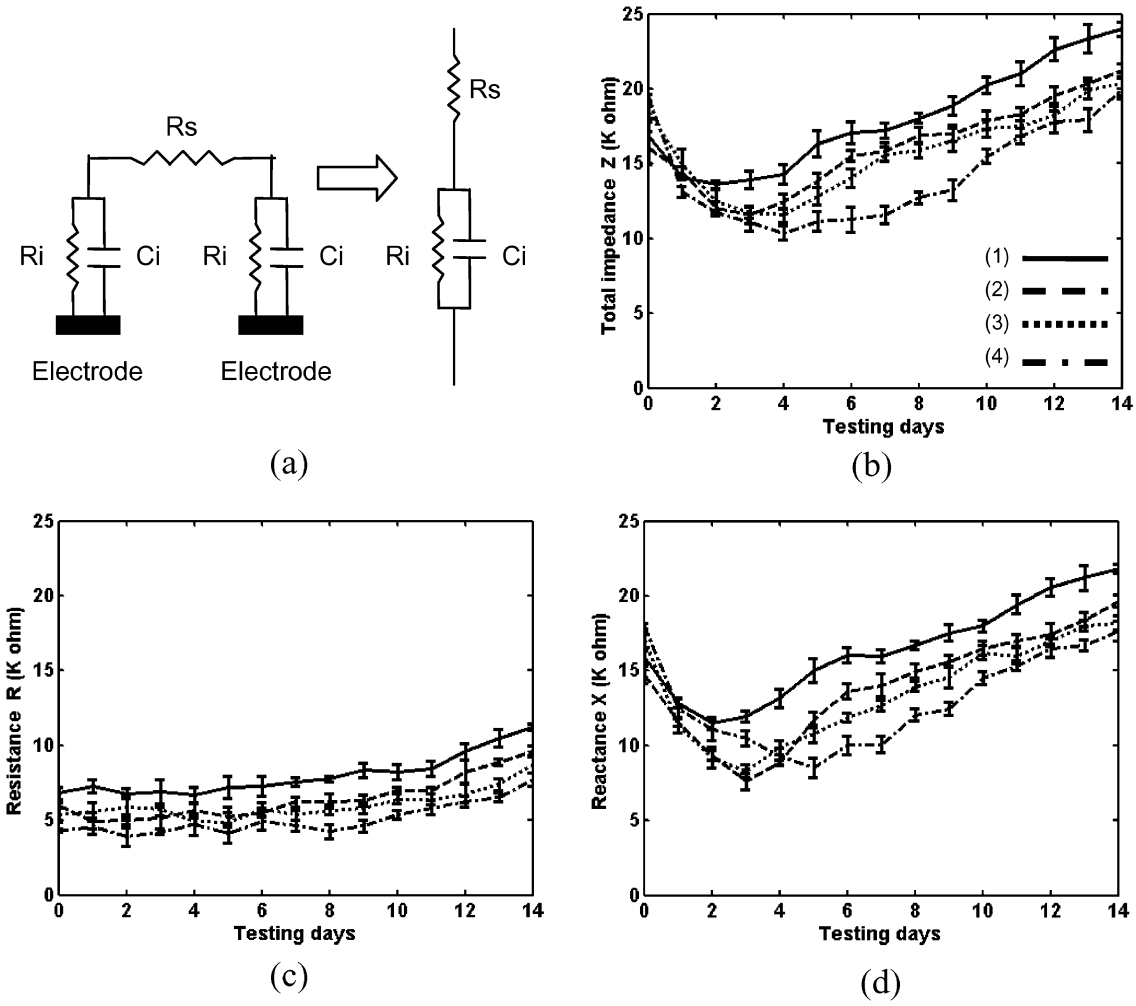

Figure 4. Total impedances were recorded from multipolar microelectrode surfaces of (1) Au/PI, (2) DDT/Au/PI, (3) HDT/Au/PI, and (4) ODT/Au/PI after immersed into saline solution containing diluted blood plasma up to 14 days. The illustration of (a) exhibited the layout of electrode impedance measurements using parallel circuit mode, and (b), (c), and (d) demonstrated the respective total impedance (Z), resistance (R), and reactance (X) measurements versus testing days, where $Z^2 = R^2 + X^2$.

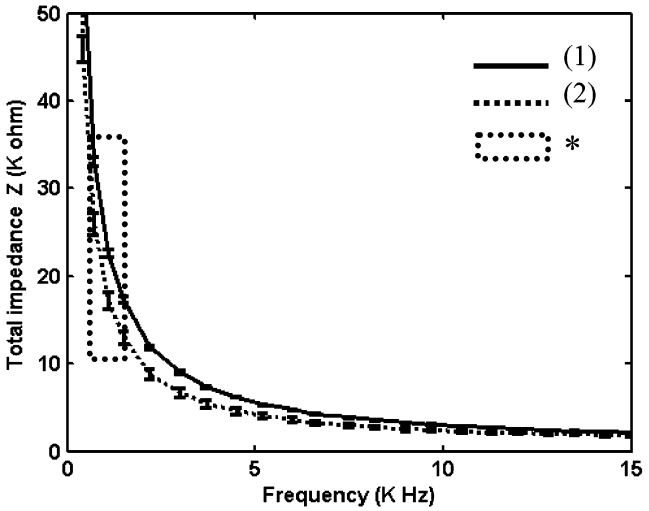

Figure 5. The total impedance versus frequency spectra for the cuff microelectrode. The impedance measurement was relatively sensitive at ≈1 kHz, located in the range of "suitable" frequencies (*). The samples for this expression were (1) Au/PI and (2) ODT/Au/PI as immersed into saline solution containing diluted blood plasma for 14 days.

the upsurge of its reactance, which was likely in association with the bulk density of adsorbates such as ions in saline solution and protein in diluted blood plasma, in the vicinity of the microelectrode surface. Figure 4b and 4d demonstrates that within the first three testing days, the SAMs modified Au/PI decreased their total impedances, whereas they constantly augmented after the fourth testing days. The decrease of reactance as well as total impedance at the initial stages could be related to the conductivity of ions in saline solution, soon after contacting with the microelectrode surface. The reaction causing such a decrease presumably depends on the ionic strength of a complex, including an electrical double layer, formed in the vicinity of the electrified microelectrode. This particular instance exhibits an analogous reaction as the illustration of the primary salt effect, one of the mechanisms by which ionic strength affects reaction kinetics. The nature of the effect is easy to understand through well-known Debye−Hückel theory, which stands to reason that the interaction is sensitive to the net force between the reacting ions. In the present case, the electrified microelectrode surface was regarded as a group of reacting ions. As a consequence, the ionic strength of the complex determined the extent of the ionic atmosphere around the charged surface, which in turn dictated the average force field in the vicinity of Au/PI surface with or without SAMs treatment.

The reaction kinetics of the electrified microelectrode surface in saline solution containing diluted blood plasma

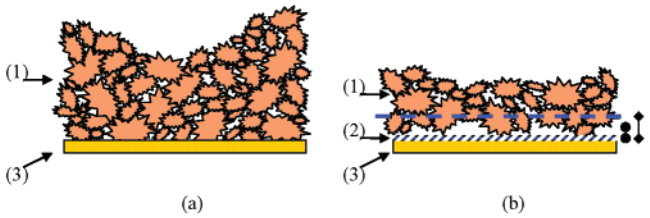

Figure 6. Schema of protein deposition upon (a) Au/PI and (b) SAMs-treated Au/PI surfaces. The protein-accumulated thickness (1) was correlated with the development of protein pileup process, which was significantly retarded for the (2) SAMs-treated film upon (3) Au/PI surface. The alkyl chains of SAMs might act as spacers (●) and form a subsequently effected depth (◆).

was complicate in determining ionic strength. In the experiment, the primary salt effect upon Au/PI surface lasted for only 2 days. It also implied that the average repulsion between blood plasma or protein and the charged surface surrounded by ions was gradually lessened. Afterward, during the next testing days, the total impedance and the reactance increased with a rate of ≈0.97 KΩ/day and ≈1.30 KΩ/day, respectively. In the thin-film SAMs treated Au/PI, the decrease of total impedance extended to 4 days, corresponding with the chain lengths of SAMs (i.e., ODT > HDT > DDT). After the fifth day, the total impedance and the reactance for the alkanethiolate SAMs/Au/PI samples increased with a rate in the range of 0.88∼1.01 KΩ/day and 0.74∼0.95 KΩ/day, respectively. With the increase of the chain lengths, the shape of the typical curves moved to the right; however, the increased rate of total impedance raised slightly. It signified that the introduction of SAMs film upon Au/PI surface was capable to extend net repulsion force with respect to protein and therefore reduce the total impedance and the reactance at the initial testing days, whereas those for Au/PI with or without SAMs treatment had a tendency to reach a maximum after a period of testing time. Overall, Au/PI surface with a long-chain SAMs treatment provided an interface or spacers to lessen the increase of total impedance or reactance as a function of testing days. This phenomenon occurred at the initial stages of electrode impedance measurement, which was

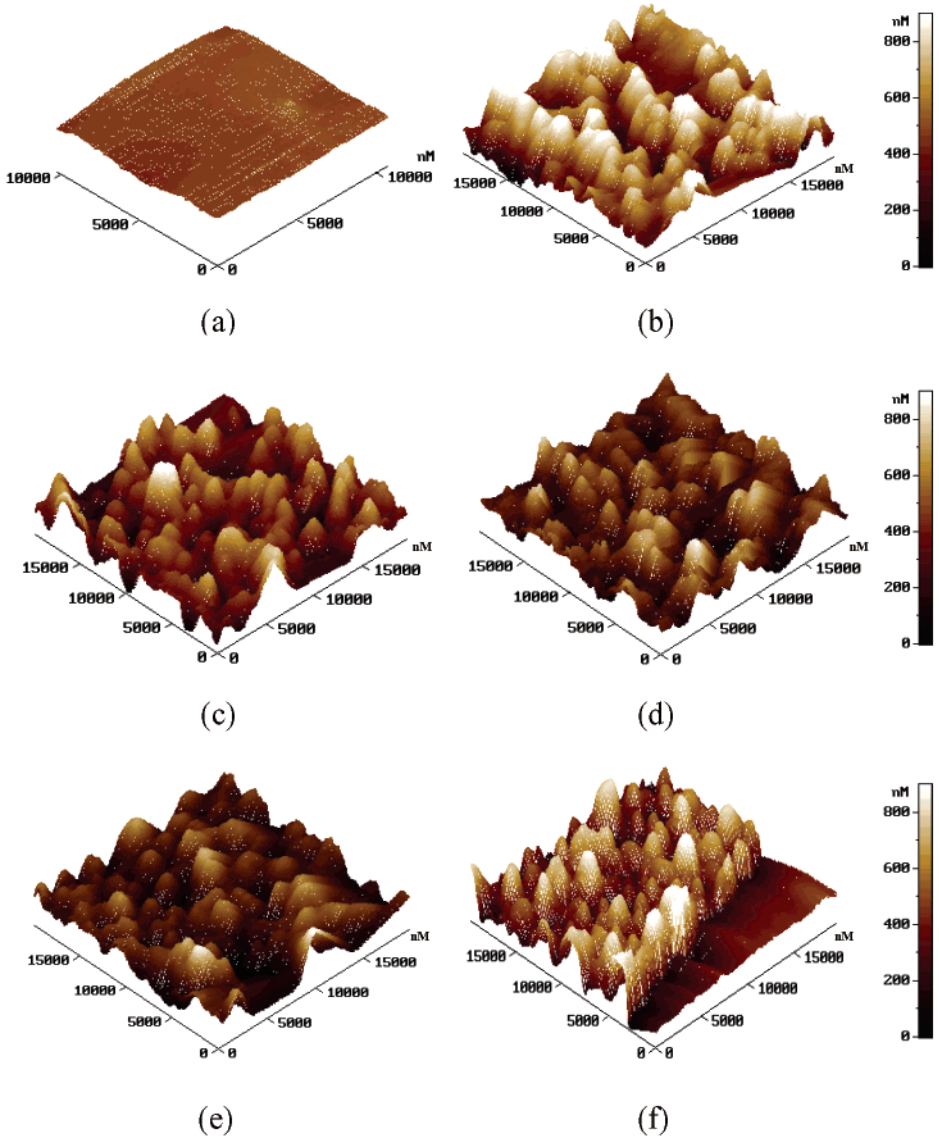

Figure 7. AFM topography of (a) ODT/Au/PI surface and protein deposition upon (b) Au/PI, (c) DDT/Au/PI, (d) HDT/Au/PI, and (e) ODT/Au/PI surfaces, and (f) an analogous (b) with a scratch-off part for the expression of measuring the protein-deposited thickness. The samples were immersed into saline solution containing dilute blood plasma for 14 days. Maxima *Z* axis scale was 800 nm.

Table 1. Thickness and Roughness of Protein-Deposited Layer Adsorbed on Au/PI without or with SAMs Treatment[a]

protein-deposited samples	thickness (nm) after 7/14 testing days	roughness (nm, Ra) after 7/14 testing days
Au/PI surface	257.9 ± 4.8/628.35 ± 21.6	74.7 ± 5.9/199.6 ± 10.7
DDT/Au/PI surface	175.3 ± 4.8/480.4 ± 15.2	51.4 ± 5.1/134.2 ± 5.9
HDT/Au/PI surface	144.9 ± 2.8/369.2 ± 6.5	46.1 ± 1.5/121.9 ± 7.7
ODT/Au/PI surface	118.4 ± 6.7/330.5 ± 7.6	37.5 ± 2.2/95.3 ± 13.4

[a] These were immersed into saline solution containing diluted blood plasma for 7 or 14 days.

also correlated with chain lengths of SAMs adsorbed upon Au/PI surface.

3.3. Kinetics of Protein Adsorption. The increase of total impedance or reactance upon the microelectrode surface, as a function of testing days, resulted from the accumulation of protein molecules on a protein-covered base. The protein pileup (or thickening) process at latter stages was roughly comparable upon various SAMs-treated surfaces but relatively higher upon the Au/PI surface. Figure 6 illustrated an accumulation or a pileup process of protein molecules upon Au/PI (Figure 6a) or a SAMs-modified (Figure 6b) surface. Form the result of AC impedance measurements, the alkanthiolate SAMs film on Au/PI surface was capable to reduce protein adsorption at the initial stages, while the long-chain SAMs surface tended to inhibit the process of accumulating protein molecules. Therefore, the differences of growing impedance as a function of testing days among Au/PI, DDT/Au/PI, HDT/Au/PI, and ODT/Au/PI were likely based on the increased thickness from protein deposition. From Figure 4b, the ODT SAMs on Au/PI could then be the most efficient surface to delay the protein accumulation process. It thus implied that analogous SAMs surfaces with different chain lengths were capable to slow the increase of electrode impedance as a function of testing days. Nevertheless, owing to the increase of protein pileup process upon an equivalent protein-deposited base, the total impedance and the reactance tended to rise in proportion to the pileup thickness of adsorbed protein. The increased rate of total impedance for the ODT SAMs on Au/PI (≈0.88 KΩ/day) climbed at the latter stages. The total impedances from different SAMs-treated surfaces in saline solution containing diluted blood plasma increased with testing days, whereas the total impedance as well as the reactance from Au/PI sample still maintained a relatively high value for the same testing day.

3.4. Surface Morphology and Adhesion of Protein on the Microelectrode Surfaces. As illustrated in Figure 6, the latter stages of protein adsorption upon a comparable base resulted in a pileup process, which tended to be developed in their preferred anchoring sites.[21] Figure 7 exhibited the AFM topography for the protein-deposited Au/PI and various SAMs-treated Au/PI surfaces, which were immersed into saline solution containing diluted blood plasma for 14 days. These protein-deposited surfaces became rough in morphology as a function of testing days, as illustrated in Figure 6. Using AFM, parts of thickness and roughness measurements on the protein-deposited Au/PI with or without SAMs treatment were listed in Table 1. Protein deposition on Au/PI surface became dense and rough after 7 or 14 days of immersing into saline solution containing diluted blood plasma, while such a process was found retarded owing to the thin-film SAMs upon Au/PI. The increase of chain length of SAMs upon Au/PI surface significantly decreased the protein-deposited thickness or thus the roughness for the analogous testing day. This implied that SAMs treatment upon Au/PI surface considerably reduced the protein deposition rate.

The processing stages in developing such deposition resulted in the increase of protein-deposited thickness and morphological changes at the protein pileup surfaces. It was very likely that SAMs adsorbed upon Au/PI surface contributed to slow the progress of protein deposition, expressed as the thickness of the layers and the roughness of the surface morphology. In accordance with the AC impedance measurements, the initial stages of protein adsorption and subsequent development of protein pileup process were therefore associated with the rise of total impedance and reactance as a function of testing time.

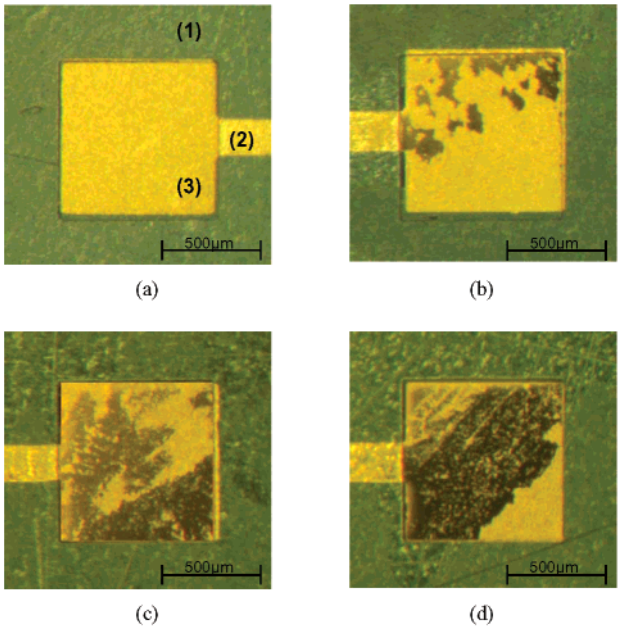

Figure 8. Protein detachment tests for the 14-day protein-deposited (a) Au/PI, (b) DDT/Au/PI, (c) HDT/Au/PI, and (d) ODT/Au/PI surfaces. The fractional coverage of residual protein upon the tested surface could be estimated. The regions marked in a were (1) protein/PI, (2) protein/PI/Au/PI, and (3) protein/Au/PI. For the contrast in region 3 of the samples b−d, the bright part was covered with protein and the dark one was the intact SAMs/Au/PI surface.

It is assumed that protein pileup process for different microelectrode surfaces, including other treatment methods, may follow a competitive model of reactions on surfaces. The rate of protein deposition upon the protein-deposited surfaces could approximate to a minimum. As a consequence, protein deposition on a chronically implanted surface with or without SAMs treatment tended to obtain an analogous protein-thickening deposition and surface morphology at their steady states. The major contribution of the alkanethiolate SAMs film was probably to create functional spacers between protein molecules and Au/PI surface. As shown in Figure 8, using saline solution to remove the accumulated protein from the protein-deposited surfaces, a great portion of them particularly upon the long-chain SAMs treated Au/PI could be easily washed away, whereas protein molecules exhibited firm adhesion upon Au/PI surface. Potentially, it is advantageous to regenerate a great portion of the SAMs-treated film on Au/PI and apply that for long-term

stimulation and recording during implantation, if an external force such as ultrasonic vibration can be exerted and reached at the interface between a living peripheral nerve and the SAMs-treated surface of Au-coated cuff-type microelectrode.

4. Conclusions

The well-ordered alkanethiolate SAMs adsorbed upon Au/PI microelectrode surface is a useful tool to slow protein adsorption process when immersed into saline solution containing dilute blood plasma. The reaction kinetics of protein accumulation upon Au/PI with or without SAMs treatment is correlated with the measurements of total impedance, resistance, reactance, and AFM topography. The increase of total impedance and reactance, as a function of testing days, resulted from the accumulation of protein molecules upon the microelectrode surface. The protein deposition rate is roughly comparable upon SAMs-treated Au/PI but relatively high upon Au/PI. The development of protein deposition on a microelectrode surface is determined by evaluating protein pileup thickness and surface morphology, which is a practical approach to predict the extent of processing stages of protein deposition as a function of testing time. Overall, SAMs treatment with longer spacers, such as ODT, on Au/PI surface is capable to supply a much efficient interface to retard protein deposition process even though a short-chain SAMs upon Au/PI significantly reduces protein deposition rate, as compared to Au/PI. Assume that eventually protein deposition rate reaches a constant value regardless of the state of a microelectrode surface. The major contribution of the alkanethiolate SAMs film is to create functional spacers between protein molecules and Au/PI surface. Particularly, the long-chain SAMs-modified film is capable of removing a significant portion of the accumulated protein from the protein-deposited surface, whereas those comparable protein molecules exhibit firm adhesion upon Au/PI surface. It is therefore advantageous to regenerate a great portion of the SAMs film adsorbed upon Au-coated nerve microelectrode and apply that for long-term stimulation and recording during implantation, if the intact part of the film acts as spacers and functions to detach the deposited protein through an external force.

Acknowledgment. This work was partly supported by National Health Research Institute of Taiwan under the contract number of NHRI-EX90-9017EP. Technical support to fabricate the nerve microelectrode was given by Micro-Nano Technology Research Center, National Cheng Kung University and Southern Region Micro-Electro-Mechanical System Research Center in Tainan, Taiwan. The authors would like to thank Mr. C.-C. Weng and Mr. Y.-T. Wu for performing HRXPS measurements at the National Synchrotron Radiation Research Center in Shinchu, Taiwan.

LA040097T